Dither signals optimization in constrained multi-agent extremum seeking control

Thiago Lima Silva * **Alexey Pavlov** *

* *Department of Geoscience and Petroleum, NTNU, 7031 Trondheim –*
Norway (e-mails: thiago.l.silva@ntnu.no, alexey.pavlov@ntnu.no)

Abstract: In this paper we consider the problem of optimization of a multi-agent system with constraints through perturbations-based extremum seeking control. We demonstrate that for such systems, effects of dither signals applied to individual agents can sum up to significant perturbations in the outputs at the overall system level despite the fact that individual dither signals can be small. These perturbations are especially detrimental in constrained outputs. To resolve this challenge, we propose a method of dither signals optimization: while maintaining persistent perturbations of individual agents, dither signals are coordinated between the agents to minimize their summed effect in constrained outputs. This problem is formulated as a computationally feasible mathematical programming problem that can be solved numerically at each time step. Combined with a constrained steady-state optimizer and a least squares-based gradient estimator, this method provides better performance than a similar perturbation-based extremum seeking scheme without dither optimization. This is demonstrated with an example on oil production optimization from a system of multiple gas-lifted wells with a total water processing constraint.

Keywords: Dither signals optimization, extremum seeking control, constrained model-free optimization

1. INTRODUCTION

Extremum seeking control (ESC) is a popular model-free optimization method that has received significant attention from the scientific community in the last two decades, see, e.g. Krstic and Wang (2000); Krstic (2000); Ariyur and Krstic (2003); Tan et al. (2008); Tan et al. (2010); Hunnekens et al. (2014); Guay and Dochain (2015); Haring (2016). It allows one to achieve automatic optimization of steady-state behavior of an unknown plant, where the steady-state behavior is quantified in terms of an a-priori unknown best measured cost function. Optimization is achieved by manipulating inputs through feedback of the plant outputs. Apart from applications to optimization of individual systems, ESC has been applied to optimization of systems consisting of multiple interconnected subsystems (possibly with a specification of the interconnection topology), resulting in a number of publications on distributed Extremum Seeking Control for multi-agent systems, see, e.g. Ye and Hu (2015); Pavlov et al. (2017); Ebegbulem and Guay (2018); Wang et al. (2019).

In practical problems it is quite often the case that while seeking an optimum, an optimizer needs to respect certain operational constraints. The attainable performance of the overall system (formulated in the form of a cost function) is in many practical cases limited by one or more constraints. For multi-agent systems, these constraints can be both on the level of individual systems (agents) or on the level of the overall multi-agent system. Results on ESC for individual constrained systems have been presented in, e.g., Dehaan and Guay (2005); Coito et al. (2005); Poveda and Quijano (2012); Dürr et al. (2013); Guay et al. (2015), while extensions to multi-agent systems (still with constraints on individual agents) have been reported in Nedic

et al. (2010); Kvaternik and Pavel (2012); Poveda and Quijano (2013); Dougherty and Guay (2016).

In a specific type of multi-agent optimization problems, namely, resource allocation problems, constraints are formulated not only on the individual systems (agents), but also on the operation of the overall system as a whole. For example, the total available resource to be allocated among the agents to achieve optimal performance of the overall system is limited, giving us a constraint on the sum of all the individual systems' inputs. At the same time, overall performance can also be limited by a constraint on the sum of the individual systems' outputs.

For multi-agent optimization problems with such overall constraints, application of perturbation-based extremum seeking control may face a challenge that is not encountered in problems with constraints only on individual agents. This challenge arises from system-wide perturbations caused by dither signals of individual subsystems (agents). In perturbation-based ESC, system's input is a sum of a fast varying dither signal (for gradient estimation of unknown functions) and a slowly-varying value adjusted by the optimizer to bring the average input value to the optimum. Dither signals are commonly chosen to have small amplitudes to extract the essentially local gradient information and to avoid large dither-induced variations in the individual system's input and output. For multi-agent optimization problems with overall system constraints, small dither-induced perturbations from individual agents can sum up to a large perturbation in the constrained inputs and outputs of the overall system. While the slowly varying components of the control inputs can converge to the constrained optimum, this large perturbation will result in persistent non-small violations of the constraints (if the optimum is at the constraint).

A practical solution to resolve this problem is to utilize virtual constraints separated from the actual constraints in the steady-state optimizer, which are to account for perturbations. While the average input values satisfy the virtual constraints, the per-

turbed values will satisfy the original constraints. However, to account for the large dither-induced perturbations in the overall system's input and output, the virtual constraints may need to be overly conservative, resulting in quite a suboptimal operation of the overall system. In applications from the oil and gas industry (we use an example of a multi-well oil production system to motivate our study), such sub-optimality will result in significant economical losses, making this conventional approach inappropriate.

In this work we present a solution to the challenge of large dither-induced perturbations in the overall constrained multi-agent system's input and output by optimizing and coordinating dither signals between individual agents. For each agent, there is quite some freedom in dither signal selection. For example, for sinusoidal dither signals, one can play with the amplitude and phase while keeping the amplitude within certain min and max bounds. These degrees of freedom have no effect on the efficiency of the gradient estimation of individual systems. The proposed solution utilizes such degrees of freedom within all the agents to minimize a steady-state dither-induced perturbations in constrained input and output of the overall system. Minimal (or, as demonstrated by simulations, negligible) dither-induced perturbations in the input and output, allow the system to operate much closer to the constraints without violating them, as, for example, compared to the method of the virtual constraints presented above. This, in turn, will result in a more economically beneficial operation of the system.

Previous works on dither signals focused on their shape, frequency and amplitude. The shape affects the convergence rate of the gradient estimator, see, e.g. Tan et al. (2008). The amplitude should allow persistence of excitation to ensure convergence to the optimum, see, e.g. Adetola and Guay (2007). The frequency should be sufficiently high to ensure time-scale separation between the dynamics of the gradient estimator, the process optimizer and the plant, see, e.g. Krstic (2000); Suttner (2019). In multi-agent systems improved performance can be achieved by re-using frequencies of agents that do not affect the other's steady-state performance significantly, see, e.g. Kutadinata et al. (2014). Note that the closest related work, see, e.g. Adetola et al. (2004), to minimization of dither signals does not apply in our case. Although that paper does focus on minimization, in some sense, of the overall dither signal, this minimization does not guarantee small values of the overall input in the infinity norm, which is essential in our application. Secondly, that work focuses only on the reduction of dither-induced variations at the input of the system, and it does not minimize the dither-induced variations in the overall output of the system, which is also very important for our application.

This work is an extension of the dither signals optimization study initiated in Silva and Pavlov (2020) to the case of constrained multi-agent ESC. While the application of ESC to constrained multi-agent systems is not new, see, e.g. Nedic et al. (2010); Kvaternik and Pavel (2012); Poveda and Quijano (2013); Dougherty and Guay (2016), the minimization of the dither-induced variations both in the input and in the output of the overall system by means of dither signals coordination for such problems is considered, to the best of the authors' knowledge, for the first time, despite its practical relevance.

The paper is organized as follows. In Section 2 we formulate the constrained optimization problem of multi-agent systems and formulate the problem of dither signals optimization. In Section 3 we present analysis and a numerical method for dither signals optimization. In Section 4 we present an overall ESC optimizer with dither signals optimization. Section 5 demon-strates application of the proposed solution to the problem of optimal gas allocation for gas-lifted wells with a constraint on the total produced water. We conclude with Section 6.

2. PROBLEM FORMULATION

In this section we firstly formulate the constrained optimization problem for a multi-agent system with overall (system-wide) constraints. Then we formulate the problem of dither signals optimization that arises in solving the first optimization problem with a perturbations-based extremum seeking control.

Let us consider N systems described by static relations:
$$y_i = f_i(u_i), \quad , y_i \in \mathbb{R}, u_i \in \mathbb{R}, \quad i = 1, \ldots, N, \quad (1)$$
with a-priori unknown strictly concave functions $f_i(u_i)$. Both u_i and y_i are available for measurements. We need to find a control algorithm for u_i to automatically maximize the following cost function:
$$Y := \sum_{i=1}^{N} f_i(u_i) \to \max \quad (2)$$
subject to input constraints on individual agents:
$$u_i^{\min} \leq u_i \leq u_i^{\max}, i = 1, \ldots, N \quad (3)$$
for some $u_i^{\max} > u_i^{\min}$, and to system-wide constraints:
$$U := \sum_{i=1}^{N} u_i \leq \mathrm{U}^{\max}, \quad (4)$$
$$W := \sum_{i=1}^{N} g_i(u_i) \leq \mathrm{W}^{\max} \quad (5)$$
for some a-priori unknown functions $g_i(\cdot)$. It is assumed that $g_i(u_i), i = 1, \ldots N$, are also measured. We assume that inequalities (3)-(5) specify a compact convex set such that the overall optimization problem (2)-(5) has a unique optimum. In addition to that we assume that the functions f_i and g_i are sufficiently smooth and that there exists a gradient search-type optimizer algorithm (called steady-state optimizer) that, given gradients of f_i and g_i, ensures convergence of control inputs $\bar{u}_i$ to the unique optimum from any initial condition $\bar{u}_i(0)$, while satisfying the constraints (3)-(5).

Extremum seeking control is a suitable tool to address the above mentioned problem. Since the gradients of f_i and g_i are generally unknown, to employ the optimizer, one needs to estimate them. The optimizer combined with the gradient estimator constitute the essence of extremum seeking control. To enable gradient estimation in perturbation-based ESC, slowly varying control inputs $\bar{u}_i$ are supplied with slowly varying value adjusted by the optimizer and a dither signal $d_i(t)$ — fast-varying perturbation signal that allows one to estimate gradients of $\frac{\partial f_i}{\partial u_i}(\bar{u}_i)$ and $\frac{\partial g_i}{\partial u_i}(\bar{u}_i)$:
$$u_i = \bar{u}_i + d_i(t), \quad i = 1 \ldots, N. \quad (6)$$
The overall effect of dither signals on the constrained variables U and W are given by
$$U = \underbrace{\sum_{i=1}^{N} \bar{u}_i}_{=:\bar{U}} + \underbrace{\sum_{i=1}^{N} d_i(t)}_{=:J_\mathrm{u}}. \quad (7)$$
$$W = \underbrace{\sum_{i=1}^{N} g_i(\bar{u}_i)}_{=:\bar{W}} + \underbrace{\sum_{i=1}^{N} g_i(\bar{u}_i + d_i(t)) - \sum_{i=1}^{N} g_i(\bar{u}_i)}_{=:J_\mathrm{g}}. \quad (8)$$

While the steady-state optimizer can handle constraints (4), (5) on the nominal values $\bar{U}$ and $\bar{W}$, the terms J_u and J_g can lead to significant variations in the actual U and W. Even when each dither signal $d_i(t)$ can be relatively small, their overall effect on U and W, especially for large N, can be quite large. In practice, this can be quite detrimental for physical equipment, since these large and relatively fast perturbations can result in increased equipment wear and reduced life-time. On the other hand, one still needs to satisfy the constraints (4), (5) in the presence of the large perturbations. To account for the perturbations, the constraints on $\bar{U}$ and $\bar{W}$ need to be made more restrictive, leading to suboptimal operation.

To minimize or avoid the dither-induced perturbations in U and W, we formulate the following dither signals optimization problem:

$$\|J_\mathrm{u}\|_\infty = \max_t \left| \sum_{i=1}^N d_i(t) \right| \to \min_{\{d_i(\cdot)\}} \tag{9}$$

$$\|J_\mathrm{g}\|_\infty = \max_t \left| \sum_{i=1}^N g_i(\bar{u}_i + d_i(t)) - g_i(\bar{u}_i) \right| \to \min_{\{d_i(\cdot)\}} \tag{10}$$

subject to constraints

$$d_i^{min} \leq \max_t |d_i(t)| \leq d_i^{max} \tag{11}$$

for some d_i^{max} and d_i^{min} that ensure the possibility to identify the gradients. Notice that condition (11) can be substituted by an appropriate persistence of excitation condition. Even though we formulate two optimization objectives (9) and (10), in practice one can either combine them into one objective, or restrict one of the cost functions by a small value, while minimizing the remaining one.

Although (10) contains unknown functions g_i, it is still possible to solve this optimization problem based on available measurements, as will be demonstrated in the next section.

3. DITHER SIGNAL OPTIMIZATION

To overcome the problem of unknown functions $g_i(u_i)$ in (10), we approximate J_g with the linear approximation of $g_i(u_i)$:

$$g_i(\bar{u}_i + d_i) - g_i(\bar{u}_i) \approx \frac{\partial g_i}{\partial u_i}(\bar{u}_i) \cdot d_i \tag{12}$$

To simplify the notation, we denote the derivative $\frac{\partial g_i}{\partial u_i}(\bar{u}_i)$ as $G_i(\bar{u}_i)$, and thus Eq. (10) becomes:

$$\|J_\mathrm{g}\|_\infty \approx \|J_\mathrm{G}\|_\infty := \max_t \left| \sum_{i=1}^N G_i(\bar{u}_i) \cdot d_i(t) \right| \to \min_{\{d_i(\cdot)\}}. \tag{13}$$

Although the gradients G_i are still unknown, they can be estimated by a gradient estimation algorithm from the measured $g_i(u_i)$. Thus, all parameters in (9) and (13) become known and we can optimize $d_i(t)$ to achieve the optimization objectives (9) and (13). Below we demonstrate this concept for the case of sinusoidal dither signals, which are often used in extremum seeking control.

The conceptual formulation of the dither signals optimization problem (9), (10), (11) can be tailored for any particular choice of dither signals. In this work, we assume sinusoidal dither signals of the following form:

$$d_i(t) = \alpha_i \sin(\omega t + \varphi_i), \quad i = 1 \ldots N \tag{14}$$

where the signal amplitude is α_i, the frequency is ω, and the phase is φ_i. The frequency ω is chosen off-line in order to achieve time-scale separation with the steady-state optimizer. The remaining parameters for optimization are the amplitudes α_i and the phases φ_i, $i = 1, \ldots N$.

After substituting $d_i(t)$ from (14) to (13) and (9), we still obtain a challenging optimization problem (nonlinear and non-convex problem) with respect to the amplitudes α_i and phases φ_i. To overcome this challenge, we utilize an equivalent parametrization proposed in Silva and Pavlov (2020):

$$d_i(t) = a_i \cdot \sin(\omega t) + b_i \cdot \sin(\omega t), \tag{15}$$

where a_i and b_i are the optimized parameters of the dither signals. The actual amplitudes α_i and phases φ_i of the signals can be obtained with the following relations:

$$\alpha_i = \sqrt{a_i^2 + b_i^2} \tag{16}$$

$$\varphi_i = \arctan \frac{b_i}{a_i} \tag{17}$$

With the new parametrization, the variations in the input and the corresponding output variation at each time step (see (9) and (13)) can be written as:

$$J_\mathrm{u} = \left(\sum_i a_i \right) \sin(\omega t) + \left(\sum_i b_i \right) \cos(\omega t) \tag{18}$$

$$J_\mathrm{G} = \left(\sum_i G_i \cdot a_i \right) \sin(\omega t) + \left(\sum_i G_i \cdot b_i \right) \cos(\omega t) \tag{19}$$

where the optimizing parameters a_i and b_i now appear linearly in the equations representing the dither-induced variations. From this, we obtain

$$\|J_\mathrm{u}\|_\infty^2 = \left(\sum_i a_i \right)^2 + \left(\sum_i b_i \right)^2 \tag{20}$$

$$\|J_\mathrm{G}\|_\infty^2 = \left(\sum_i G_i \cdot a_i \right)^2 + \left(\sum_i G_i \cdot b_i \right)^2. \tag{21}$$

Individual constraints (11) can be captured taking into account the relation:

$$\max_t |d_i(t)|^2 = a_i^2 + b_i^2. \tag{22}$$

3.1 Formulation of the dither signals optimization problem

With the expressions for total variations and maximal amplitudes in (20)–(22), we can formulate the dither signals optimization problem in a form that can be solved with standard numerical optimization methods, see, e.g. Nocedal and Wright (2006) . The dither optimization problem consists in optimally selecting the tuning parameters a_i and b_i for the dither signals in (15) such that the equations are satisfied:

$$\left(\sum_i G_i \cdot a_i \right)^2 + \left(\sum_i G_i \cdot b_i \right)^2 \to \min_{\{a_i, b_i\}} \tag{23}$$

$$\left(\sum_i a_i \right)^2 + \left(\sum_i b_i \right)^2 \leq \delta_\mathrm{in}^2 \tag{24}$$

$$(d_i^{min})^2 \leq a_i^2 + b_i^2 \leq (d_i^{max})^2, \quad i = 1 \ldots N \tag{25}$$

Note that instead of two minimization objectives (9) and (13), we select to minimize only (13) (or, equivalently (21)), while restricting (9) (or, equivalently, (20)) by a small value δ_in^2.

The optimization problem (23)-(25) depends on the slowly-varying $\bar{u}_i$ as parameters. Thus, the solution to the optimization

problem will also change with $\bar{u}_i$ ($\bar{u}_i$ are adjusted by the steady-state optimizer). To avoid fast variations of the dither parameters a_i and b_i, we impose additional constraints on their subsequent changes Δa_i and Δb_i:

$$|\Delta a_i|^2 \leq \Delta a^{\max} \quad i = 1, \ldots N, \tag{26}$$

$$|\Delta b_i|^2 \leq \Delta b^{\max}, \quad i = 1, \ldots N, \tag{27}$$

for some $\Delta a^{\max}$ and $\Delta b^{\max}$.

If the gradients G_i or their estimates are available, we can solve the optimization problem (23)-(27) numerically at each time step. With exact knowledge of the gradients G_i, it can be shown that the left-hand sides in both (20) and (21) can be set to zero by proper conditioning of amplitudes and phases in individual non-zero dither signals. This is possible for $N \geq 3$. The proof of this statement goes beyond the objectives of this publication and is left out for a journal version of the paper.

4. CONSTRAINED ESC WITH DITHER OPTIMIZATION

In this section we combine the dither signals optimization scheme developed in the previous section with a steady-state optimizer and gradient estimator. The overall scheme is illustrated in Figure 1. It represents a further development of the ESC scheme described in Silva and Pavlov (2020) including system-wide operational constraints. For simplicity of presentation, in this section we consider optimization problem (2) only with constraint (5). Including all the other constraints will only make the optimizer more elaborate, while the concept of dither signals optimization for constrained ESC (which is the main contribution of this paper) remains the same.
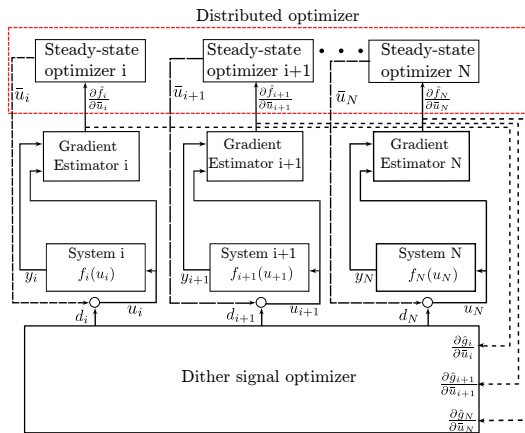

Fig. 1. Extremum-Seeking Scheme.

For every system i in Figure 1, the input signal u_i is the sum of the nominal input $\bar{u}_i$ and a dither signal $d_i(t)$. The gradient estimator calculates the estimates the gradients $\frac{\partial \hat{f}_i}{\partial \bar{u}_i}$ and $\frac{\partial \hat{g}_i}{\partial \bar{u}_i}$ from the measured u_i and outputs $f_i(u_i)$ and $g_i(u_i)$. The steady state optimizer performs slow adaptations of the nominal inputs $\bar{u}_i$ such that the system is driven towards the optimal solution while avoiding violating the operational constraint.

4.1 Augmented cost function

To develop a steady-state optimizer for the optimization problem (2) with constraint (5), we transform, using a barrier method, see, e.g. Nocedal and Wright (2006), the constrained optimization problem (2), (5) into an unconstrained problem.

The constraint (5) is included in the form of barrier functions in an augmented cost function. The barrier function penalizes the constraint violation in the objective such that the solution of the unconstrained problem is driven towards the neighborhood of the minimizer $\mathbf{u}^* = (u_1^*, \ldots, u_N^*)$ of the constrained problem.

A common choice for barrier functions is the logarithmic barrier because it possesses the desired property of going to minus infinity as the constraint becomes nearly active, see, e.g. Nocedal and Wright (2006). Using the logarithmic barrier, we define an augmented objective function which encodes the objective (2) and the constraint (5) as follows:

$$J^{\mathrm{A}}(\mathbf{u}) := \sum_i f_i(u_i) - \mu \log \left(W^{\max} - W(\mathbf{u}) \right) \rightarrow \max \tag{28}$$

where $W(\mathbf{u}) = \sum_i g_i(u_i)$ and $\mu > 0$ is a strictly positive penalty. Notice that the unconstrained minimization of the augmented cost J_A approaches the solution of (2) and (5) as the penalty $\mu \rightarrow 0$.

4.2 Steady-state optimizer

After the transformation with the logarithmic barrier, the optimization problem consists in determining the input signals u_i such that the augmented cost function $J^{\mathrm{A}}(\mathbf{u}, \mu)$ is maximized. In extremum-seeking control the steady-state optimizer is responsible for the slower adaptations performed in the input signals towards the optimal solution. For the optimizer, in our case, we choose the simple gradient search scheme:

$$\dot{\bar{u}}_i = \gamma_i \cdot \left[\frac{\partial f_i}{\partial u_i}(\bar{u}_i) - \left(\frac{\mu}{W^{\max} - W(\bar{u})} \right) \cdot \frac{\partial g_i}{\partial u_i}(\bar{u}_i) \right] \tag{29}$$

where the tuning parameter γ_i is the optimizer gain of the controller i.

4.3 Least squares gradient estimator

The steady-state optimizer relies on accurate estimates of the gradients $\frac{\partial f_i}{\partial \bar{u}_i}$ and $\frac{\partial g_i}{\partial \bar{u}_i}$ to perform the adaptations in the input signals towards the optimum. As proposed in Silva and Pavlov (2020), we utilize a static estimator to estimate these gradients, thereby avoiding the interplay between the dither signals optimizer and dynamics of the gradient estimator.

The gradient estimator calculates the gradient and a smoothened value of the function based on the 1st-order least-square fits of stored data from previous time steps in a sliding window (Hunnekens et al., 2014). A sliding window stores data from the past T_w seconds from previous time steps. The gradient p_i is obtained from the least-squares fit $p_i \cdot u_i(t) + q_i$ of the window data at time step t as the solution of the following convex optimization problem:

$$\min_{p_i, q_i} \int_{-T_\mathrm{w}}^{0} \left(f_i(t + \tau) - (p_i \cdot u(t + \tau) + q_i) \right)^2 \cdot d\tau. \tag{30}$$

We select the window size to be an integer multiplier of the dither signal wave period. Its size determines the smoothness of the gradient estimates (in case of noisy measurements) as well as the delay of the estimates: the bigger the window is, the smoother and more delayed is the estimation.

The value of $W(\bar{u}) = \sum_i g_i(\bar{u}_i)$ is not measured. We can estimate $g_i(\bar{u}_i)$ for all i (and, thus, $W(\bar{u})$) from the measured $u_i = \bar{u}_i + d_i(t)$ and the corresponding $g_i(u_i(t))$ using the same least squares estimator as for calculating the gradients of $g_i(u_i)$.

4.4 Dither signal optimizer

The dither signal optimizer is based on (23)-(27) where instead of true gradients $G_i = \frac{\partial g_i}{\partial u_i}(\bar{u}_i)$ we utilize their estimates $\hat{G}_i$:

$$J_{\mathrm{G}} = \left(\sum_i \hat{G}_i \cdot a_i\right)^2 + \left(\sum_i \hat{G}_i \cdot b_i\right)^2 \to \min_{\{a_i, b_i\}} \quad (31)$$

$$\left(\sum_i a_i\right)^2 + \left(\sum_i b_i\right)^2 \le \delta_{\mathrm{in}}^2 \quad (32)$$

$$(d_i^{min})^2 \le a_i^2 + b_i^2 \le (d_i^{max})^2, \quad i = 1 \dots N \quad (33)$$

$$|\Delta a_i|^2 \le \Delta a^{\max} \quad i = 1, \dots N, \quad (34)$$

$$|\Delta b_i|^2 \le \Delta b^{\max}, \quad i = 1, \dots N, \quad (35)$$

5. SIMULATION EXAMPLE

We consider an application example from the petroleum industry to assess the performance of the proposed method. In some oil production systems, specially in the early stage of production, the reservoir pressure is enough to lift up the fluids from the wells to the platform naturally. However, when the reservoir pressure depletes and its pressure is not sufficient to ensure an economically viable operation, some artificial-lift support is required. A widely used artificial-lift method is called gas-lift. It consists of injecting pressurized gas down-hole into the well such that the injected gas reduces the fluid density, leading to a reduction in the hydrostatic pressure in the vertical column of the well, which yields an increase in the well production rate. If the gas injection rate becomes too large, the friction caused by the additional gas flow becomes greater than the hydrostatic pressure reduction improvement, and therefore the production begin to decrease. There is a function that relates the oil rate to the gas injection rate in a well, usually referred to as production curve or gas-lift performance curve. Is is typically a concave curve ($y = f(u)$) with a unique maximum point u^*, where u is gas injection rate and y is the oil production rate. In addition to oil wells produce gas and water also.

The wells typically produce to a common top-side processing facility, where the total produced gas is processed in a shared compressor, as shown in Figure 2. A subsea manifold gathers and directs the production from all the wells to the processing facilities for separation. A fraction of the gas is pressurized to be injected into the wells for gas-lift support. The optimization problem can be formulated as an optimal resource allocation problem: how to split the total gas available for gas-lift among the production wells such that the total oil production is maximized ? Typically, there is an additional constraint on the total water production, as platforms water processing capacity is limited.

In our simulation study, we consider a system with $N = 5$ wells such that their gas-lift injection rates are the input signals $u_i, i = 1, \dots 5$. The production curves relating the oil production rates of the wells to given gas injection rates are concave functions of the form:

$$f_i(u_i) = c_{1,i} \times 10^{-7} \cdot u_i^4 + c_{2,i} \times 10^{-4} \cdot u_i^3 +$$
$$c_{3,i} \times 10^{-2} \cdot u_i^2 + c_{4,i} \cdot u_i + c_{5,i}, \quad (36)$$

where $c_{1,i}$, $c_{2,i}$, c_3, i, $c_{4,i}$, and $c_{5,i}$ are the coefficients of the production curve of well i. The production curves are depicted in Figure 3. They are used in the simulations, but are unknown to the ESC controller. The unconstrained maximum of the curves is $(u_1^*, u_2^*, u_3^*, u_4^*, u_5^*) \approx (83.75, 98.31, 64.81, 108.62, 79.68)$. The water cut of the wells were set to $w_1 = 0.08$, $w_2 =$
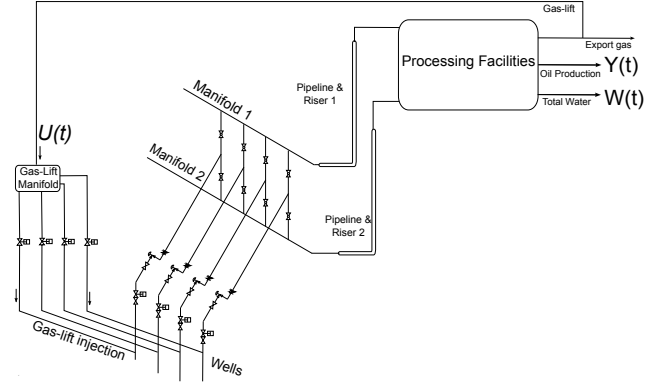

Fig. 2. A production gathering network with 4 gas-lifted wells and subsea manifolds (Silva and Pavlov, 2020).

Table 1. Production curves coefficients

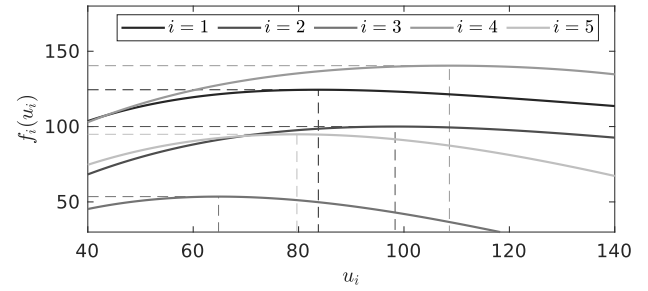|	well 1	well 2	well 3	well 4	well 5
$c_{1,i}$	-3.9	-1.3	-1.2	-4	-1.4
$c_{2,i}$	2.1	1	1	1.8	1
$c_{3,i}$	-4.3	-2.8	-2.8	-3.6	-2.9
$c_{4,i}$	3.7	3.1	3.1	3.5	3
$c_{5,i}$	12	-17	-17	-16	-5

Fig. 3. Gas-lift performance curves (Silva and Pavlov, 2020).

0.15, $w_3 = 0.16$, $w_4 = 0.22$, $w_5 = 0.4$. The water produced by each well g_i can be obtained from the oil production f_i with a simple relation:

$$g_i = f_i \cdot \frac{w_i}{1 - w_i}, \forall i \in 1, \dots, N. \quad (37)$$

Although the proposed ESC scheme is capable of handling multiple constraints, we focus on the output constraint on the total water handling capacity (5). Thus, we apply the developed extremum-seeking control to steer the input signals u_i towards the optimal value of the augmented cost function in (28).

The tuning parameters of the extremum-seeking control are set to $\mu = 0.05$, $\omega_i = 0.75$, and $\gamma_i = 0.3$, $\forall i \in 1, \dots, N$. The initial conditions for the input signals are $u_1(0) = 50$, $u_2(0) = 70$, $u_3(0) = 100$, $u_4(0) = 70$, and $u_5(0) = 50$. The total water handling capacity is set to $W^{\max} = 138$, which ensures the constraint activation at the optimal solution.

The ESC scheme was implemented in Simulink and Matlab R2018b. The scheme is implemented in Simulink, while the least-squares filter and the dither signal optimizer are external classes embedded into the scheme. The time step was set to $T_s = 0.1$, and we chose the window size to 3 times the wave period of the dither signals, i.e., $\lceil 3 \times (2\pi/\omega_i)/T_s \rceil$. The dither signal optimizer is formulated in CasADI v3.4.5 (Andersson et al., 2019), and the dither optimization problem is solved with the nonlinear solver IPOPT (Wächter and Biegler, 2006). The

bounds for the constraints are set to $\delta_{\text{in}} = 10^{-5}$, $d_i^{\min} = 0.5$, $d_i^{\max} = 2.5$, $\Delta a_i^{\max} = \Delta b_i^{\max} = 0.8$.

The performance of the proposed ESC scheme with dynamically optimized dither signals is compared to a similar scheme with fixed dither signals. While in the first case the amplitudes and phases are calculated online by the dither signal optimizer, in the latter the dither signals have the same amplitude and phases, $\alpha_i = 1.5$ and $\phi_i = 0$, $\forall i = 1, \ldots, N$. The input signals $u_i, i = 1, \ldots, N$ with the proposed scheme are shown in Figure 4. The nominal input signals $\bar{u}_i$ converge to values in the

Fig. 4. Input signals.

neighborhood of the constrained optimum $(u_1^*, u_2^*, u_3^*, u_4^*, u_5^*)$ $\approx (83.78, 98.14, 64.87, 107.4, 57.95)$.

The amplitudes and phases of the optimized dither signals are shown in Figures 5 and 6, respectively. The adaptations in the
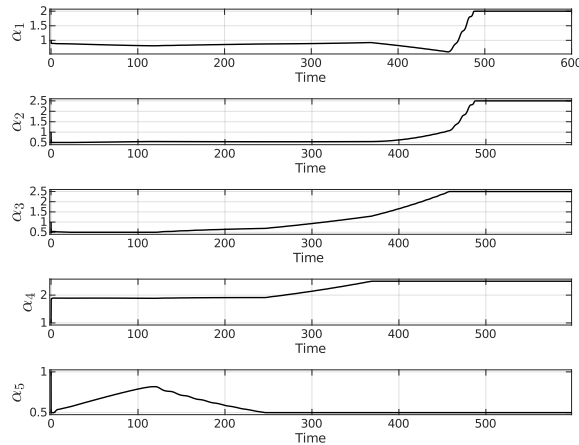

Fig. 5. Dither amplitudes.

dither signals occur mainly before the maximum is achieved in each production curve individually, and when the water handling constraint becomes nearly active. The rate of change in the adaptations depend on the the upper bounds that are chosen for the continuity constraints in Eqs (26) and (27). To ensure feasibility of the adaptations, such bounds should be consistent with the steady-state optimizer gains.

The total oil production obtained with the ESC scheme with optimized dither signals and with fixed signals are shown in Figure 7. Notice that the nominal inputs $\bar{u}_i$ for both the ESC scheme with optimized and fixed dither signals converge to a value near to the constrained optimum $\sum_{i=1}^{N} f_i(u_i^*) = 507.73$. To illustrate the performance of dither signal optimization,
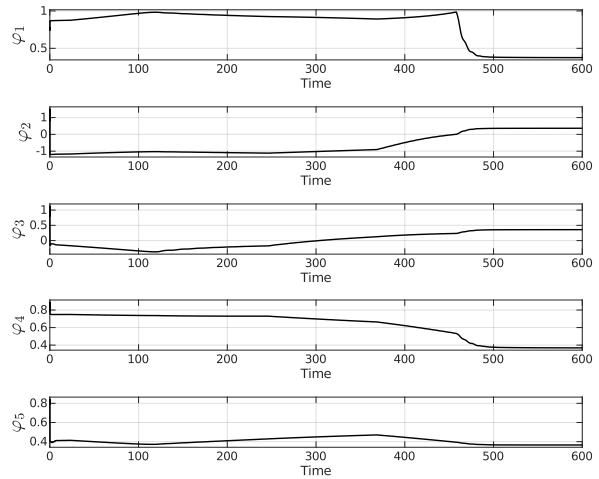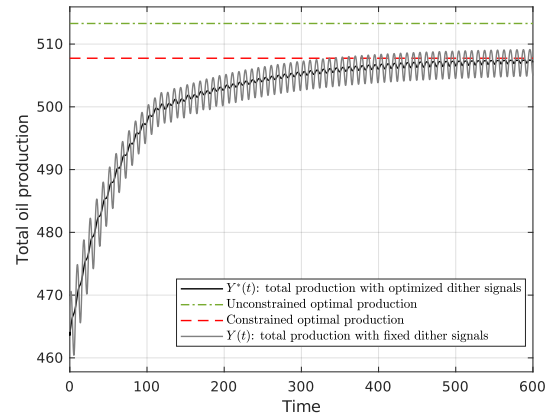

Fig. 6. Dither phases.

Fig. 7. Objective function.

we compare the total water produced with both schemes in Figures 8. The ESC scheme with optimized dither signals
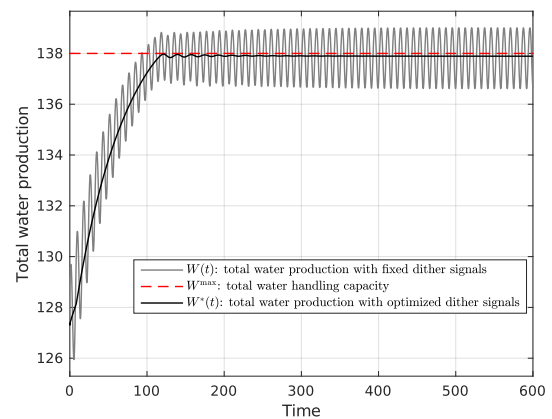

Fig. 8. Total water production.

successfully honor the output constraint while operating near the upper bound. On the other hand, because of the large dither-induced variations in the water produced, the scheme with fixed signals violates the constraint. One could argue that it would be possible to include a virtual constraint to avoid such violations, however this would result in significant economic

losses due to an overly conservative operation. The total output variations in the ESC scheme with fixed dither signals J_G are considerably larger ($\approx 100\times$) than the output variations with optimized signals J_G^*. In the latter, the estimated and the actual total variations are negligible, bounded to 10^{-2}. Further, while the amplitude of the total input variations with fixed dithers are large ($|J_U| \approx 30$), the total input variations with optimized dither signals is quite small, bounded to $\delta_{in} \leq 10^{-5}$.

6. CONCLUDING REMARKS

In this paper we have considered the problem of optimization of a multi-agent system with constraints using the paradigm of extremum seeking control. We have demonstrated that in a perturbation-based extremum seeking control the effects of dither signals from multiple agents can sum up to significant perturbations in the constrained outputs. To overcome this problem, we have presented a method for dynamic optimization of dither signals that minimizes (or practically cancels) the effect of dither-induced perturbations from the individual agents on constrained outputs, while maintaining persistent perturbations on each individual agent. To demonstrate the proposed method, we have coupled it with a constrained steady-state optimizer and a least-squares gradients estimator. The performance of the overall scheme has been demonstrated with application to an optimization problem from the oil and gas industry. The new proposed controller with dither signals optimization has demonstrated much better performance than the same controller without dither optimization. Theoretical proofs of the presented approach are left out for a journal publication. Further work will include extension of the presented results to multiple constraints, and application of the proposed method in more interesting examples where the agents have coupled-dynamics.

REFERENCES

Adetola, V., DeHaan, D., and Guay, M. (2004). Adaptive extremum-seeking receding horizon control of nonlinear systems. In *Amer. Control Conf., 2004. Proc. of the 2004*, volume 4, 2937–2942. IEEE.

Adetola, V. and Guay, M. (2007). Parameter convergence in adaptive extremum-seeking control. *Automatica*, 43(1), 105 – 110.

Andersson, J.A.E., Gillis, J., Horn, G., Rawlings, J.B., and Diehl, M. (2019). CasADi – A software framework for nonlinear optimization and optimal control. *Math. Program. Comput.*, 11(1), 1–36.

Ariyur, K.B. and Krstic, M. (2003). *Real-time optimization by extremum-seeking control*. John Wiley & Sons.

Coito, F., Lemos, J., and Alves, S. (2005). Stochastic extremum seeking in the presence of constraints. *IFAC Proc. Volumes*, 38(1), 276–281.

Dehaan, D. and Guay, M. (2005). Extremum-seeking control of state-constrained nonlinear systems. *Automatica*, 41(9), 1567–1574.

Dougherty, S. and Guay, M. (2016). An extremum-seeking controller for distributed optimization over sensor networks. *IEEE Trans. on Autom. Control*, 62(2), 928–933.

Dürr, H.B., Zeng, C., and Ebenbauer, C. (2013). Saddle point seeking for convex optimization problems. *IFAC Proc. Volumes*, 46(23), 540–545.

Ebegbulem, J. and Guay, M. (2018). Resource allocation for a class of multi-agent systems with unknown dynamics using extremum seeking control. In *2018 IEEE Conf. on Decis. and Control (CDC)*, 2496–2501.

Guay, M. and Dochain, D. (2015). A time-varying extremum-seeking control approach. *Automatica*, 51, 356 – 363.

Guay, M., Moshksar, E., and Dochain, D. (2015). A constrained extremum-seeking control approach. *Int. J. of Robust and Nonlinear Control*, 25(16), 3132–3153.

Haring, M.A.M. (2016). *Extremum-seeking control: convergence improvements and asymptotic stability*. Ph.D. thesis, NTNU.

Hunnekens, B., Haring, M., van de Wouw, N., and Nijmeijer, H. (2014). A dither-free extremum-seeking control approach using 1st-order least-squares fits for gradient estimation. In *53rd IEEE Conf. on Decis. and Control*, 2679–2684.

Krstic, M. (2000). Performance improvement and limitations in extremum seeking control. *Systems & Control Letters*, 39(5), 313 – 326.

Krstic, M. and Wang, H.H. (2000). Stability of extremum seeking feedback for general nonlinear dynamic systems. *Automatica*, 36(4), 595 – 601.

Kutadinata, R.J., Moase, W.H., and Manzie, C. (2014). Dither re-use in nash equilibrium seeking. *IEEE Trans. on Autom. Control*, 60(5), 1433–1438.

Kvaternik, K. and Pavel, L. (2012). An analytic framework for decentralized extremum seeking control. In *2012 Amer. Control Conf. (ACC)*, 3371–3376. IEEE.

Nedic, A., Ozdaglar, A., and Parrilo, P.A. (2010). Constrained consensus and optimization in multi-agent networks. *IEEE Trans. on Autom. Control*, 55(4), 922–938.

Nocedal, J. and Wright, S. (2006). *Numerical optimization*. Springer Science & Business Media.

Pavlov, A., Haring, M., and Fjalestad, K. (2017). Practical extremum-seeking control for gas-lifted oil production. In *Decis. and Control (CDC), 2017 IEEE 56th Annual Conf. on*, 2102–2107. IEEE.

Poveda, J. and Quijano, N. (2012). A shahshahani gradient based extremum seeking scheme. In *2012 IEEE 51st IEEE Conf. on Decis. and Control (CDC)*, 5104–5109. doi: 10.1109/CDC.2012.6426134.

Poveda, J. and Quijano, N. (2013). Distributed extremum seeking for real-time resource allocation. In *2013 Amer. Control Conf.*, 2772–2777. IEEE.

Silva, T.L. and Pavlov, A. (2020). Dither signal optimization for multi-agent extremum seeking control. In *2020 Proc. of the 20th European Control Conf. (ECC)*.

Suttner, R. (2019). Extremum seeking control with an adaptive dither signal. *Automatica*, 101, 214 – 222.

Tan, Y., Moase, W.H., Manzie, C., Nei, D., and Mareels, I.M.Y. (2010). Extremum seeking from 1922 to 2010. In *Proc. of the 29th Chinese Control Conf.*, 14–26.

Tan, Y., Nei, D., and Mareels, I. (2008). On the choice of dither in extremum seeking systems: A case study. *Automatica*, 44(5), 1446 – 1450.

Wächter, A. and Biegler, L.T. (2006). On the implementation of an interior-point filter line-search algorithm for large-scale nonlinear programming. *Math. Program.*, 106(1), 25–57.

Wang, D., Chen, M., and Wang, W. (2019). Distributed extremum seeking for optimal resource allocation and its application to economic dispatch in smart grids. *IEEE Trans. on Neural Networks and Learning Systems*, 30(10), 3161–3171.

Ye, M. and Hu, G. (2015). A distributed extremum seeking scheme for networked optimization. In *2015 54th IEEE Conf. on Decis. and Control (CDC)*, 4928–4933.